INTERNATIONAL JOURNAL FOR NUMERICAL METHODS IN FLUIDS
Int. J. Numer. Meth. Fluids 2004; **46**:345–359 (DOI: 10.1002/fld.725)

Dynamical systems-based optimal control of incompressible fluids

Michael Hintermüller, Karl Kunisch*,†, Yulian Spasov‡ and Stefan Volkwein

Institut für Mathematik und Wissenschaftliches Rechnen, Karl-Franzens-Universität Graz, Heinrichstrasse 36, A-8010 Graz, Austria

SUMMARY

For optimal control problems related to fluid flow the choice of an adequate cost functional for suppression of vortices is of significant importance. In this research we propose a cost functional based on a local dynamical systems characterization of vortices. The resulting functional is a non-convex function of the velocity gradient tensor. The resulting optimality system describing first order necessary optimality conditions is derived, a possible strategy for numerical realization of the optimal control problem is provided and a numerical feasibility study is conducted. Copyright © 2004 John Wiley & Sons, Ltd.

KEY WORDS: optimal control; incompressible flow; dynamical systems

1. INTRODUCTION

The objective of this work is the introduction of a novel optimal control formulation for the reduction and possibly extinction of vortices in an incompressible fluid and the description of a feasibility study of the proposed methodology. Optimal control is based on the minimization of a cost functional

$$J(y,u)=J_1(y)+\beta J_2(u) \tag{1}$$

over a set U of admissible controls u. Here $y=y(t,x)$ denotes the velocity vector of the fluid at time $t>0$ and location x in the spatial domain Ω. Further, $\beta>0$ stands for the control costs. The controls u can be body forces or action like blowing or suction along the boundary of Ω. Alternatively, the control action on the fluid can be enforced in a more indirect manner

*Correspondence to: Karl Kunisch, Institut für Mathematik und Wissenschaftliches Rechnen, Karl-Franzens-Universität Graz, Heinrichstrasse 36, A-8010 Graz, Austria.
†E-mail: karl.kunisch@uni-graz.at
‡Present address: Swinden Technology Centre, Corus, Rotherham, S60 3AR, U.K.

Contract/grant sponsor: Fonds zur Förderung der wissenschaftlichen Forschung; contract/grant number: SFB 03; Optimierung und Kontrolle

Published online 16 July 2004

Received 7 April 2003
Revised 25 November 2003

like heating or cooling. In many cases a proper choice for J_2 is given by

$$J_2(u) = \frac{1}{2}\int_0^T \int_{\Omega_c} |u(t,x)|^2 \,\mathrm{d}x\,\mathrm{d}t \tag{2}$$

where T is the control horizon and $\Omega_c \subset \bar{\Omega}$ the support of the controller. It expresses the fact that applying control requires resources and in mathematical terms—after possible modifications in case of boundary control—it typically guarantees the existence of a minimizer of J in (1) over $u \in U$.

The choice of J_1 is significantly more involved. It must be governed by the physical goal of describing vortices and by numerical feasibility considerations. The following choices can be found in the literature and have been proven to be successful in the sense of reduction or elimination of spiraling streamlines in specific numerical experiments:

$$J_1(y) = \frac{1}{2}\int_0^T \int_{\Omega} |\mathrm{curl}\, y|^2 \,\mathrm{d}x\,\mathrm{d}t \tag{3}$$

$$J_1(y) = \frac{1}{2}\int_0^T \int_{\Omega} |y - y_{\mathrm{Stokes}}|^2 \,\mathrm{d}x\,\mathrm{d}t \tag{4}$$

$$J_1(y) = \frac{1}{2}\int_0^T \int_{\Omega} |g(y)|^2 \,\mathrm{d}x\,\mathrm{d}t \tag{5}$$

where g is a problem-dependent function of the state y. In case of channel flow, with the longitudinal extension along the x_1-axis, for example, one would choose $g(y) = \min(0, y_1)$ [1]. The functional in (4) is of tracking type, with y_{Stokes} the solution of the Stokes equation and otherwise the same problem data (without control) as that for obtaining y. Minimizing the square of the vorticity as in (3) was considered in References [2–4], for example. As with (4) and (5) formulation (3) is a practical choice, but it has short-comings. These include that $|\mathrm{curl}\, y|$ does not identify vortex cores in shear flow, especially if the background shear is comparable to the vorticity within vortex [5]. From the numerical control point of view the main difficulty involved in realizing the minimization of J with J_1 as in (3) is given by the fact that the adjoint equation, which characterizes the gradient of J with respect to u, involves inhomogeneous terms of the form $(\mathrm{curl}^\star)\,\mathrm{curl}$, with $\mathrm{curl}^\star$ the adjoint operation of curl. As a consequence the solutions to the adjoint equation can be fairly rough and good adjoint solvers are essential. Turning to (4) and (5) next, both these functionals do not attempt to quantify vorticity of the fluid in terms of intrinsic properties of the velocity field y or pressure p. Thus, while vortices may be reduced by minimizing J with (4) and (5) this can be at the cost of suppressing features of the non-linear flow which ought to sustain. Let us, however, emphasize one highly desirable property of cost (4) from the numerical optimization point of view. The second derivative of the cost at a control u in directions $(\delta u, \delta u)$ is given by

$$\begin{aligned} J''(u)(\delta u, \delta u) = &\int_0^T \int_{\Omega} (|y'(u)\delta u|^2 + (y(u) - y_{\mathrm{Stokes}})y''(u)(\delta u, \delta u))\,\mathrm{d}x\,\mathrm{d}t \\ &+ \beta \int_0^T \int_{\Omega_c} |\delta u|^2 \,\mathrm{d}x\,\mathrm{d}t \end{aligned} \tag{6}$$

where y' and y'' denote the first and second derivatives, respectively. Numerical methods are strongly influenced by positive definiteness of the Hessian which, by (6) is likely to hold for small residue problems where $|y(u) - y_{\text{Stokes}}|$ is small. Further tracking-type formulations with the aim of stabilization and drag reduction were investigated in e.g. References [6–9]. We also refer to References [10, 11] for proceedings publications which cover many important aspects in the area of flow control.

In this work we shall attempt to obtain a proper definition for J_1, serving the purpose of penalizing 'vorticity', by connecting it to the long-lasting question of what constitutes a vortex. In Reference [5] a list of intuitively suggestive, yet inadequate choices is provided. These include vorticity magnitude measured by $|\text{curl}\, y|$ for reasons already discussed above, path—and streamlines since they are not Galilean invariant and moreover difficult to quantify within an optimal control formulation, and finally local pressure minima, since there can be pressure minima without vortex cores.

A promising approach for the description of vortices or eddies consists of a local analysis based on dynamical systems characterized by the flow $y(x)$. Subsequent linearization of the flow around stationary points allows to use the qualitative theory of linear dynamical systems. In the case of two-dimensional flows phase plane analysis is readily available from text book literature, see e.g. Reference [12], for the three-dimensional case we refer to References [13–15], for example. Given the velocity field $y = y(t,x)$, the location x of a particle, which is at x_0 at $t = t_0$, is given as the solution to the dynamical system

$$\begin{aligned} \frac{\mathrm{d}}{\mathrm{d}t} x(t) &= y(t, x(t)), \quad t > t_0 \\ x(t_0) &= x_0 \end{aligned} \tag{7}$$

Let $\bar{x}$ denote a critical point of (7) in the sense that $y(t,\bar{x}) = 0$ for all $t \geqslant t_0$. Expanding the right-hand side of (7) in terms of x up to order one and taking t_0 as a reference time we have

$$\begin{aligned} \frac{\mathrm{d}}{\mathrm{d}t}(x(t) - \bar{x}) &= \nabla y(t_0, \bar{x})(x(t) - \bar{x}) \\ x(t_0) &= x_0 \end{aligned} \tag{8}$$

The qualitative behaviour of (8) is fully described by the spectral properties of the velocity gradient tensor $\nabla y(t_0,\bar{x})$. To simplify notation we set $A = \nabla y(t_0,x)$ and introduce its symmetric and antisymmetric parts $S = \frac{1}{2}(A + A^{\mathrm{T}})$ and $T = \frac{1}{2}(A - A^{\mathrm{T}})$, referred to as strain and rotation tensor, respectively. In case of three-dimensional flow the characteristic equation of A is given by

$$\lambda^3 - (\operatorname{tr} A)\lambda^2 + \tfrac{1}{2}((\operatorname{tr} A)^2 - \operatorname{tr} A^2)\lambda - \det A = 0$$

where $\operatorname{tr} A$ stands for the trace of A. Since $\operatorname{tr} A = 0$ for incompressible fluids the characteristic equation reduces to

$$\lambda^3 - \tfrac{1}{2} \operatorname{tr} A^2 \lambda - \det A = 0$$

Let $Q = -\frac{1}{2} \operatorname{tr} A^2$ and define the discriminant

$$D = (\tfrac{1}{2} \det A)^2 + (\tfrac{1}{3} Q)^3$$

If $D>0$ then A has one real and two complex-conjugate eigenvalues. Based on these quantities three types of definitions for the existence of vortices are found in the literature. In References [13, 14] vortex cores are related to regions with complex eigenvalues of ∇y. In terms of linear dynamical systems complex eigenvalues correspond to centres and foci, see Reference [12], and in view of (7), (8) this suggests that the local streamline pattern is closed or forms spirals in a reference frame moving with the particle. In Reference [16] an eddy is defined as a region where Q is positive with pressure which is below the ambient value. The third definition is based on the strain and rotational tensors and defines a vortex core as a connected region within which the symmetric matrix S^2+T^2 has two negative eigenvalues, [5]. Respective merits and differences among the three definitions are analysed in Reference [5]. All three are Galilean invariant and each one of them, with different degree of complexity, can be used as the basis for defining the J_1-part of the cost functional for an optimal control problem.

We turn to the two-dimensional case. In this case the velocity gradient is of the form

$$\nabla y = \begin{pmatrix} a & b \\ c & -a \end{pmatrix} \tag{9}$$

and the eigenvalues of ∇y are complex if and only if $\det \nabla y>0$. It is simple to argue that the second and third definitions above as well predict a vortex in regions where

$$\det \nabla y>0$$

For two-dimensional flows this considerations suggests, to choose

$$J_1(y)=\alpha\int_0^T\int_{\Omega_0} h(\det \nabla y(t,x))\,\mathrm{d}x\,\mathrm{d}t \tag{10}$$

where Ω_o is the region within which it is desired to suppress vortices, and h is positive whenever its argument is positive. To motivate a specific choice for h we return to the local linear system analysis. Expanding (7) at $(t_0,\bar{x})$ we have

$$\begin{aligned} \frac{\mathrm{d}}{\mathrm{d}t}(x(t)-\bar{x}) &= y(t_0,\bar{x})+A(x(t)-\bar{x}), \quad t>t_0 \\ x(t_0) &= x_0 \end{aligned} \tag{11}$$

where $A := \nabla y(t_0,\bar{x})$ is of form (9). Hence assuming that $\det A\neq 0$ there exists a regular matrix B such that

$$C := B^{-1}AB = \begin{pmatrix} 0 & \omega_1 \\ -\omega_2 & 0 \end{pmatrix}$$

with $\omega_i>0$. Introducing the new variable $z(t)=B^{-1}(x(t)-\bar{x})$ and setting $f=B^{-1}y(t_0,\bar{x})$, we have

$$\frac{\mathrm{d}}{\mathrm{d}t}z(t)=Cz(t)+f, \quad t>t_0$$

$$z(t_0)=B^{-1}(x_0-\bar{x})$$

The solution to this system is given by $z(t)=\mathrm{e}^{C(t-t_0)}(z(t_0)+C^{-1}f)-C^{-1}f$, and hence the solution to (11) is given by

$$x(t)=B\mathrm{e}^{C(t-t_0)}(z(t_0)+C^{-1}f)+\bar{x}-BC^{-1}f \tag{12}$$

Since

$$\mathrm{e}^{Ct}=\begin{pmatrix}\cos\left(\sqrt{\omega_1\omega_2}t\right) & \sin\left(\sqrt{\omega_1\omega_2}t\right)\\ -\sqrt{\frac{\omega_2}{\omega_1}}\sin\left(\sqrt{\omega_1\omega_2}t\right) & \sqrt{\frac{\omega_2}{\omega_1}}\cos\left(\sqrt{\omega_1\omega_2}t\right)\end{pmatrix}$$

the trajectories described by (12) are closed curves (centres). The lengths of their periods decreases as $\det A=\omega_1\omega_2$ increases. This suggests to choose h as a monotonically increasing function of time. To allow differentiability of the cost, h is chosen as C^1-function. This results in a possible choice for h given by

$$h(s)=\begin{cases}0 & \text{if } s<-\delta\\ \dfrac{s^2}{2\delta}+s+\dfrac{\delta}{2} & \text{if } -\delta\leqslant s\leqslant 0\\ s+\dfrac{\delta}{2} & \text{if } 0\leqslant s\end{cases} \tag{13}$$

for fixed, small $\delta>0$.

Let us briefly describe the remainder of the paper. In Section 2, we describe the two-dimensional model problem that we shall use to validate the proposed approach for optimization-based vortex reduction. Further the adjoint-based gradient representation is given. Relevant aspects for numerical optimization are summarized in Section 3. The fourth section contains numerical results and comparisons.

2. ADJOINT-BASED OPTIMAL CONTROL

Let Ω be a bounded spatial two-dimensional domain with boundary Γ. By $y=(y_1,y_2)$ we denote the velocity of the fluid in the directions $x=(x_1,x_2)$ and p denotes its pressure. The controlled time-dependent Navier–Stokes equations on the time–space cylinder $Q=(0,T)\times\Omega$, $T>0$, are given by

$$y_t-\frac{1}{Re}\Delta y+(y\cdot\nabla)y+\nabla p=\mathscr{B}u \quad \text{in } Q \tag{14a}$$

$$-\operatorname{div} y=0 \quad \text{in } Q \tag{14b}$$

where $u\in U$ is the control variable, U is the space of controls, and $\mathscr{B}: U\to L^2(Q)$ is a bounded linear operator. Further Δ denotes the component-wise Laplacian $\sum_{j=1}^{2}\partial^2 y_i/\partial x_j^2$, $(y\cdot\nabla)y$ stands for the vector with components $\sum_{j=1}^{2} y_j\partial y_i/\partial x_j$ and $Re>0$ is the Reynolds number. The function $\mathscr{B}u\in L^2(Q)$ represents a volume force. In our numerical examples the

control acts on a subset Ω_c of Ω. In this case $\mathscr{B}$ is the extension-by-zero operator, i.e. $\mathscr{B}u = u$ in Ω_c and $\mathscr{B}u = 0$ in $\Omega \backslash \Omega_c$. At $t = 0$ the initial condition

$$y(0,x) = y_\circ(x) \quad \text{for all } x \in \Omega \tag{14c}$$

is imposed, where $y_\circ$ is a given function on Ω. On the lateral boundary $\Sigma = (0,T) \times \Gamma$ we prescribe inhomogeneous Dirichlet conditions

$$y = g \quad \text{on } \Sigma \tag{14d}$$

where g is a fixed function satisfying

$$\int_0^T \int_\Gamma g \cdot n \, \mathrm{d}s \, \mathrm{d}t = 0$$

where n is the outward normal on Γ. Next we introduce the cost functional, which is motivated by the discussion of Section 1. For positive scalars α and β we define

$$J(y,u) = \alpha \int_0^T \int_{\Omega_o} h(\det \nabla y) \, \mathrm{d}x \, \mathrm{d}t + \frac{\beta}{2} \|u\|_U^2$$

with $\Omega_o \subseteq \Omega$ and h as in (13). Let Γ_o denote the boundary of Ω_o and set

$$\tilde{\Gamma}_o = \Gamma_o \backslash \Gamma$$

The optimal control problem that we consider has the form

$$\min J(y,u) \quad \text{such that } (y,p,u) \text{ solves (14)} \tag{P}$$

Let (y^*, p^*, u^*) denote a local solution to (P). Such a solution must satisfy the first order optimality conditions, referred to as the optimality system. To formally derive this system we introduce

$$\mathscr{L}(y,p,u,\xi,\pi) = J(y,u) + \int_0^T \int_\Omega \left(y_t - \frac{1}{Re} \Delta y + (y \cdot \nabla) y + \nabla p - \mathscr{B}u \right) \xi \, \mathrm{d}x \, \mathrm{d}t$$

$$+ \int_0^T \int_\Omega \pi \operatorname{div} y \, \mathrm{d}x \, \mathrm{d}t$$

Taking derivatives with respect to y, p, u, ξ, π we obtain the optimality system in the primal variables (y,p,u) and the adjoint variables (ξ, π), where for convenience we drop the superscripts *:

$$y_t - \frac{1}{Re} \Delta y + (y \cdot \nabla) y + \nabla p = \mathscr{B}u \quad \text{in } Q \tag{15a}$$

$$-\operatorname{div} y = 0 \quad \text{in } Q \tag{15b}$$

$$y = g \quad \text{on } \Sigma \tag{15c}$$

$$y(0,\cdot) = y_\circ \quad \text{on } \Omega \tag{15d}$$

$$-\xi_t - \frac{1}{Re}\Delta\xi + (\nabla y)^{\mathrm{T}}\xi - (y\cdot\nabla)\xi + \nabla\pi = R(y) \quad \text{in } Q \tag{15e}$$

$$-\operatorname{div}\xi = 0 \quad \text{in } Q \tag{15f}$$

$$\xi = 0 \quad \text{on } \Sigma \tag{15g}$$

$$\xi(T,\cdot) = 0 \quad \text{in } \Omega \tag{15h}$$

$$\beta u - \mathscr{B}^{\star}\xi = 0 \quad \text{in } U \tag{15i}$$

Here, $\mathscr{B}^{\star}: L^2(Q) \to U$ denotes the adjoint of the operator $\mathscr{B}$, $((\nabla y)^{\mathrm{T}}\xi)_i = \sum_{j=1}^{2}(\partial y_j/\partial x_i)\xi_j$, and the right-hand side in (15e) is given by

$$R(y) = -\alpha\begin{pmatrix} -\operatorname{curl}(h(\det\nabla y)\nabla y_2) + \chi_{[0,T]\times\tilde{\Gamma}_\circ} h'(\det\nabla y)(\frac{\partial y_2}{\partial x_2} - \frac{\partial y_2}{\partial x_1}) \\ \operatorname{curl}(h(\det\nabla y)\nabla y_1) - \chi_{[0,T]\times\tilde{\Gamma}_\circ} h'(\det\nabla y)(\frac{\partial y_2}{\partial x_2} - \frac{\partial y_2}{\partial x_1}) \end{pmatrix}$$

where $\chi_{[0,T]\times\tilde{\Gamma}_\circ}$ denotes the characteristic function of the set $[0,T]\times\tilde{\Gamma}_\circ$.

Introducing the reduced cost functional $\hat{J}: U \to \mathbb{R}$ by

$$\hat{J}(u) = J(y(u), u)$$

where $y(u)$ solves (14) for the control $u \in U$, we obtain from (15) that the gradient of the reduced cost functional at u in direction $\delta u \in U$ is given by

$$\langle \hat{J}'(u), \delta u\rangle_U = \langle \beta u - \mathscr{B}^{\star}\xi, \delta u\rangle_U = \langle \beta u, \delta u\rangle_U - \int_0^T \int_\Omega \xi \mathscr{B}\delta u \,\mathrm{d}x\,\mathrm{d}t$$

where ξ is computed from (15).

3. ASPECTS OF NUMERICAL OPTIMAL CONTROL

Our numerical approach is based on the reduced problem

$$\text{minimize} \quad \hat{J}(u) := J(y(u), u) \quad \text{over } u \in U \tag{16}$$

where y corresponds to the solution of (14). Problem (16) is solved by a Polak–Ribiere type conjugate gradient algorithm (CG-algorithm) combined with the strong Wolfe–Powell line search procedure for computing appropriate step-sizes along the CG search direction in every iteration; see References [17, 18]. The Polak–Ribiere method has the advantage that it performs a soft reset whenever the CG search direction yields no significant progress. This can be seen from the fact that given d^k, the CG search direction of the previous iteration, the next search direction is computed by means of

$$d^{k+1} = -\nabla\hat{J}(u^{k+1}) + \tilde{\beta}_k d^k \tag{17}$$

with

$$\tilde{\beta}_k = \frac{\langle \nabla \hat{J}(u^{k+1}), \nabla \hat{J}(u^{k+1}) - \nabla \hat{J}(u^k) \rangle_U}{\|\nabla \hat{J}(u^k)\|_U^2}$$

If it happens that u^k and u^{k+1} are very close, then $\tilde{\beta}_k \approx 0$ and, hence, the steepest descent part in the equation for d^{k+1} dominates. In addition, motivated by References [19, 20] we use

$$\beta_k = \max\{\tilde{\beta}_k, 0\}$$

i.e. whenever $\tilde{\beta}_k$ is negative we perform a reset by using the steepest descent direction. We further perform a reset if d^{k+1} is not a descent direction, i.e. when $\langle \nabla \hat{J}(u^{k+1}), d^{k+1} \rangle_U \geqslant 0$. This is necessitated by the line search rule.

Due to the fact that the gradient computation depends on the quality of the solution of the adjoint system, the implementation of the line search has to be done carefully. In fact, we implemented the following version of the strong Wolfe–Powell rule by utilizing error tolerances $\tau_1^k, \tau_2^k > 0$:

$$\hat{J}(u^k + v_k d^k) \leqslant \hat{J}(u^k) + \sigma v_k \langle \nabla \hat{J}(u^k), d^k \rangle_U + \tau_1^k$$

$$|\langle \nabla \hat{J}(u^k + v_k d^k), d^k \rangle_U| \leqslant -\rho \langle \nabla \hat{J}(u^k), d^k \rangle_U + \tau_2^k$$

with τ_1^k, τ_2^k given by

$$\tau_1^k = \tau_M(1 + |\hat{J}(u^k + v_k d^k)| + |\hat{J}(u^k)| + |\langle \nabla \hat{J}(u^k), d^k \rangle_U|)$$

$$\tau_2^k = \tau_M(|\langle \nabla \hat{J}(u^k), d^k \rangle_U| + |\langle \nabla \hat{J}(u^k + v_k d^k), d^k \rangle_U|)$$

Here $\tau_M > 0$ denotes a small tolerance of the order of the round-off error. Typical values for σ, ρ are $\sigma = 10^{-4}$, $\rho = 10^{-1}$.

Let us turn towards the termination criteria used to stop the CG-algorithm. Based on the error analysis and the arguments given in Reference [21] we used the conditions

$$|\hat{J}(u^k) - \hat{J}(u^{k-1})| \leqslant \varepsilon_{\hat{J}}(1 + |\hat{J}(u^k)|) \tag{18}$$

$$\|u^k - u^{k-1}\|_U \leqslant \sqrt{\varepsilon_{\hat{J}}}(1 + \|u^k\|_U) \tag{19}$$

$$\|\nabla \hat{J}(u^k)\|_U \leqslant \sqrt[3]{\varepsilon_{\hat{J}}}(1 + |\hat{J}(u^k)|) \tag{20}$$

for termination. Motivated by the accuracy of the adjoint solver we choose $\varepsilon_{\hat{J}} = 10^{-6}$ or 10^{-7}. In many test runs the criterion (20) was satisfied last.

4. NUMERICAL RESULTS

Here we present a numerical example by which the applicability of the proposed method is tested. As a test example we chose the flow in a 2D lid-driven cavity [22, 23]. This flow

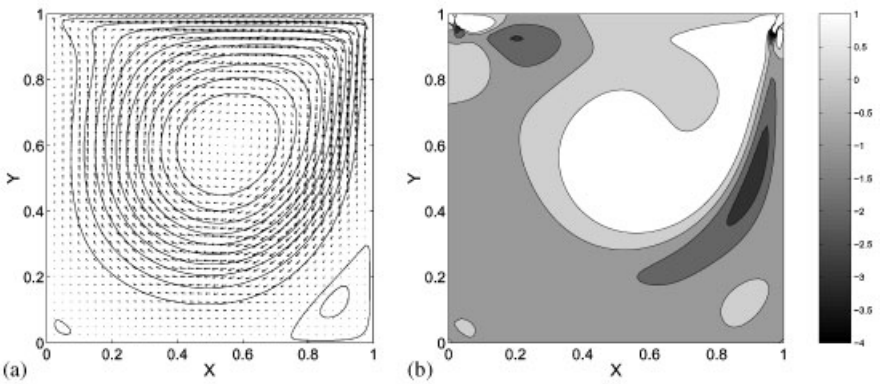

Figure 1. Lid-driven cavity flow at $Re = 400$: (a) stream function and velocity vectors; and (b) levels of $\det \nabla y$. Note that in the oval regions near the bottom corners $\det \nabla y > 0$.

has unambiguous and easy to pose boundary conditions and possesses important features of a real flow: boundary layers, core vortex and secondary vortices. These features are illustrated in Figure 1(a) by a stream function (Ψ) and velocity vectors plot for $Re = 400$. Most of the cavity is occupied by the primary vortex (PV) which is driven by the moving lid. The PV induces the bottom-left (BL) and bottom-right (BR) vortices. These vortices are also illustrated in Figure 1(b) by a contour plot of $\det \nabla y$.

Our control objective is to reduce the BR vortex. For this purpose we consider the control and observation domains $\Omega_o = \Omega_c = (0.75, 1) \times (0, 0.25)$, which are a subset of the region $\Omega = (0, 1) \times (0, 1)$ occupied by the flow. Let Γ, Γ_o and Γ_c denote the respective boundaries. The optimization horizon is given by $T = 1$.

4.1. Discretization

The controlled Navier–Stokes (14a) and continuity (14b) equations are discretized in space by means of a staggered-grid control-volume approach [24]. A fifth-order upwind finite difference scheme is applied to the convection terms whereas a fourth-order centred scheme is used for the diffusion terms. Continuity is enforced through a SIMPLE-like scheme [24] where a discrete Poisson equation is iteratively solved by means of the conjugate gradient method [25]. An explicit first-order Euler scheme is used to integrate the discrete momentum conservation equations in time. The adjoint equations (15e) and (15f) are solved using the same approach, accounting for the fact that the time integration is backwards in time. The time step is chosen small enough to guarantee both time accuracy and convergence of the solutions of the primal and adjoint systems.

The solution of the primal system is validated in Figure 2 by comparing our results with results of Reference [22]. It can be seen that an excellent agreement between the present and benchmark profiles holds. A standard check of the solution of the optimality system (15) is to track the flow to the Stokes flow. In this case $J_1(y)$ has the form given by (4). The results for $Re = 400, \alpha = 10^{-2}$, grid resolution 81×81 and time step $\delta t = 7.5 \times 10^{-3}$ are presented in Figure 3. Figure 3(a) shows that J, J_1, J_2 are converged within 15 iterations, while $\|\nabla J\|$ is further reduced about two orders of magnitude before the convergence criteria is satisfied.

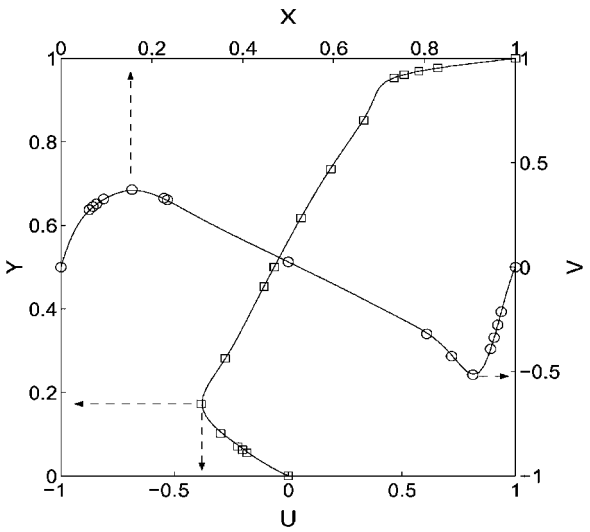

Figure 2. Lid-driven cavity flow at $Re = 1000$. Comparison of our velocity profiles (obtained on a 161×161 grid) $U|_{X=0.5}$ and $V|_{Y=0.5}$ (lines) with correspondent benchmark velocity profiles (□ and ○) from Reference [22].

Inspection of the adjoint and control fields revealed that the changes in u are small after the 15th iteration, while ξ continues to change up to the 50th iteration. Note that the value of $\|\nabla J\|$ is approximately four orders of magnitude smaller than J_2. This explains the small changes of J_1 and J_2 corresponding to big changes in $\|\nabla J\|$ after the 15th iteration. Comparing Figure 3(c) and 3(d) one can see that the control force (Figure 3(b)) successfully tracks the flow to the Stokes flow.

4.2. Reduction of the BR vortex

Before presenting the numerical results, we give the values of some parameters used in the numerical solution of the optimality system. The stopping tolerance ε_j is chosen in such a way that further iterations do not lead to significant changes in u and y. The typical value is $\varepsilon_j = 10^{-7}$.

The regularization parameter δ takes a value $\delta = 10^{-4}$ which approximately corresponds to the accuracy of the discretization for the grids used. Values $0 \leqslant \delta \leqslant 10^{-3}$ are also tested but no significant differences in the results are found.

A typical value for the cost is $\beta = 10^{-2}$. For a cheaper control (β smaller) the BR vortex of the controlled flow is generally weaker. However no significant differences between the results were found for $\beta \leqslant 10^{-2}$. The weight α of J_1 is taken to be $\alpha = 1$ if not stated otherwise.

The success of the minimization procedure depends on the gradient algorithm used to solve the optimality system (15). For example, by using the steepest descent method for $Re = 400$ combined with the Armijo's line search we obtained $\kappa \approx 8$, where

$$\kappa = \frac{\max_{\Omega_o} \Psi_{\text{uncontrolled}}}{\max_{\Omega_o} \Psi_{\text{controlled}}}$$

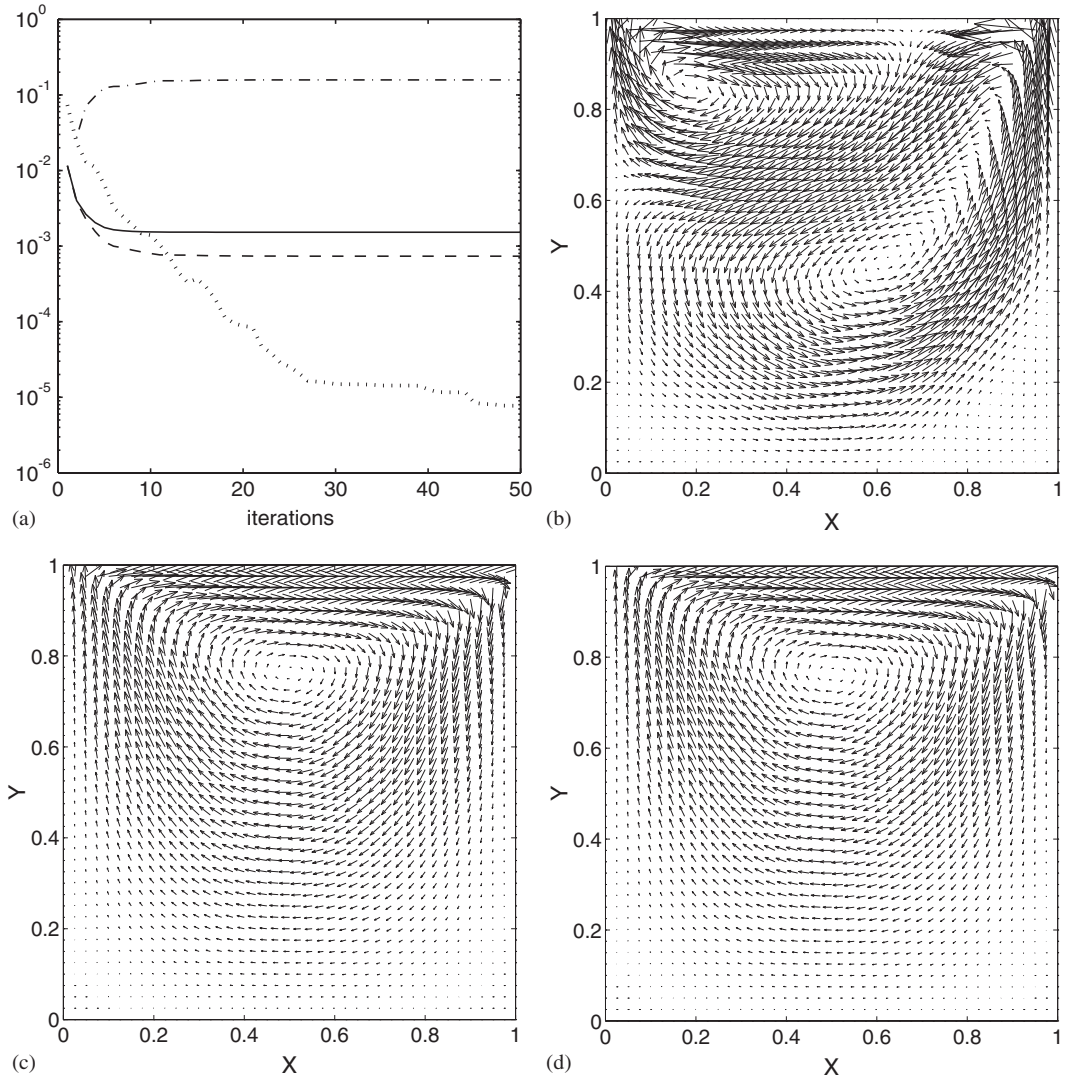

Figure 3. Tracking to Stokes flow for $Re = 400$ on a 81×81 grid: (a) convergence with the number of CG iterations: — J, −− J_1, ·− $J_2, \cdots \|\nabla J\|$; (b) control force at $t = 0.15$; (c) target flow (Stokes flow); and (d) controlled flow at $t = 0.8$.

at $t = 0.8$. For the Polak–Ribiere CG method combined either with the Wolfe–Powell or with the Armijo's line search $\kappa \approx 20$. Results with Wolfe–Powell line search are shown in Figure 4. Figure 4(a) presents the velocity vectors and stream function of the uncontrolled flow. An analogous plot of the controlled flow is presented in Figure 4(b). It can be seen that the control force shown in Figure 4c counteracts the BR vortex. Although the BR vortex is not completely suppressed its reduction is evident.

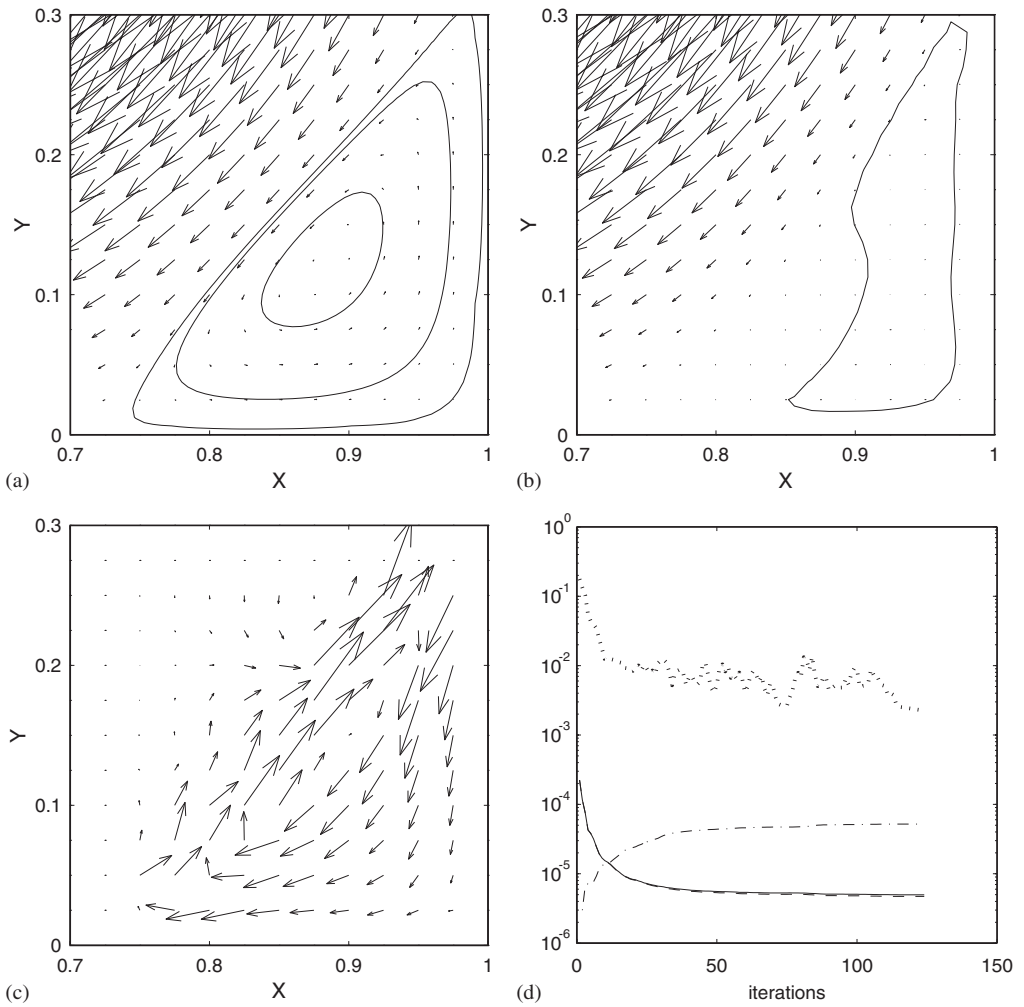

Figure 4. Results for $Re = 400$ and $\varepsilon = 1$: (a) uncontrolled flow: levels of Ψ $[5 \times 10^{-6}, 10^{-4}, 5 \times 10^{-4}]$ and velocity vectors; (b) controlled flow: a level of Ψ $[5 \times 10^{-6}]$ and velocity vectors at $t = 0.8$ (note that the higher levels of Ψ are not present in Ω_o because of the reduction of Ψ); (c) control force at $t = 0.8$; and (d) convergence with the number of CG iterations: — J, – – J_1, ·– J_2, $\cdots \|\nabla J\|$.

If the weight α of J_1 is increased by choosing $\alpha = 10$ then $\kappa \approx 10^2$. Results for $\alpha = 100$ are shown in Figure 5. It can be seen that the BR vortex is completely suppressed. It is interesting to note that if the tracking type functional $J_1(y) = \frac{1}{2} \int_0^T \int_\Omega |y - y_{\text{Stokes}}|^2 \, \mathrm{d}x \, \mathrm{d}t$ is used to suppress the BR vortex the control cost (J_2) is an order of magnitude larger.

We further checked the performance of the method for a higher value of the Reynolds number, namely $Re = 1000$. The results are depicted in Figure 6. Figure 6(b) shows that the BR vortex is suppressed in the observation region. The level of Ψ in the upper right corner

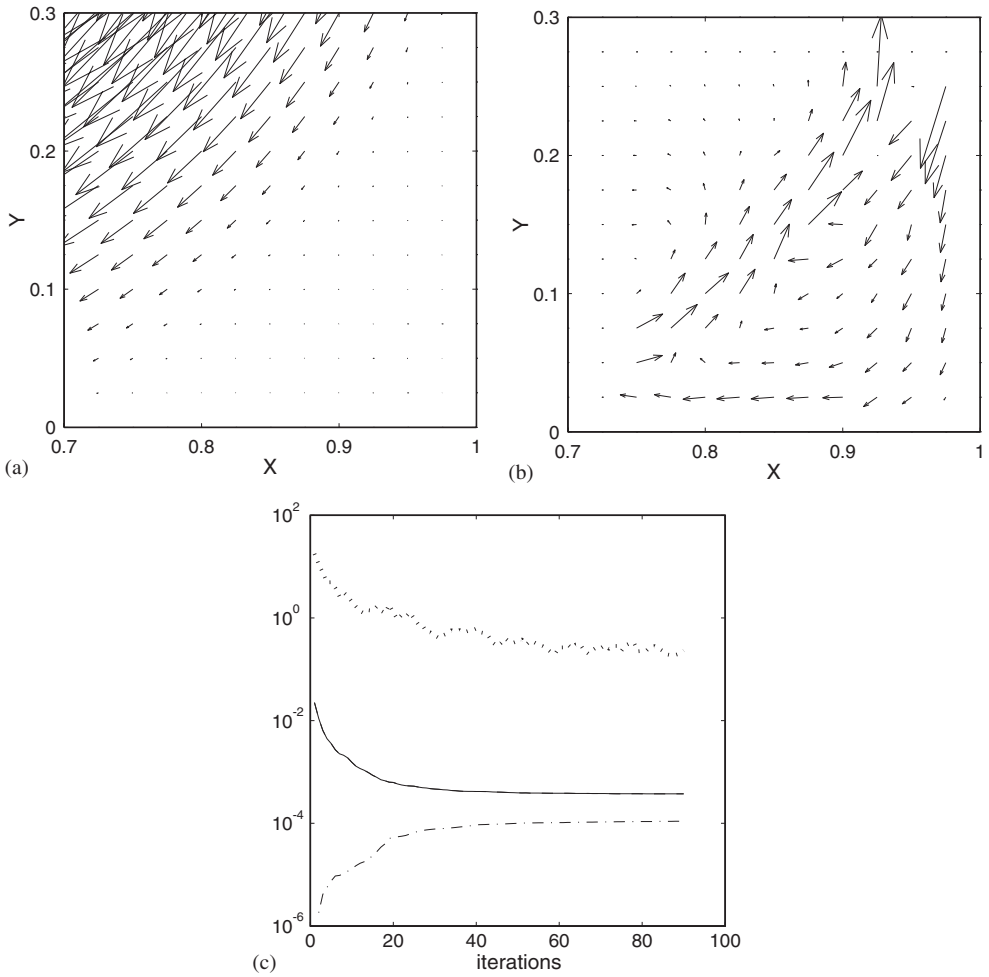

Figure 5. Results for $Re = 400$ and $\varepsilon = 100$: (a) controlled flow: levels of Ψ $[5 \times 10^{-6}, 10^{-4}, 5 \times 10^{-4}]$ and velocity vectors at $t = 0.8$ (note that the levels of Ψ are not present in Ω_o because of the reduction of the Ψ); (b) control force at $t = 0.8$; and (c) convergence with the number of CG iterations: — J, -- J_1, ·– $J_2, \cdots \|\nabla J\|$. (Note that the values of J and J_1 are very close so that they are visually indistinguishable on this plot.)

of Figure 6(b) is outside of Ω_o. The control force is depicted in Figure 6(c) and Figure 6(d) shows that the solution of the optimality system (15) is converged.

5. SUMMARY AND CONCLUSIONS

A cost functional based on phase plane analysis involving the velocity gradient tensor of the fluid is proposed for the reductions of vortices in optimal control-based formulations of

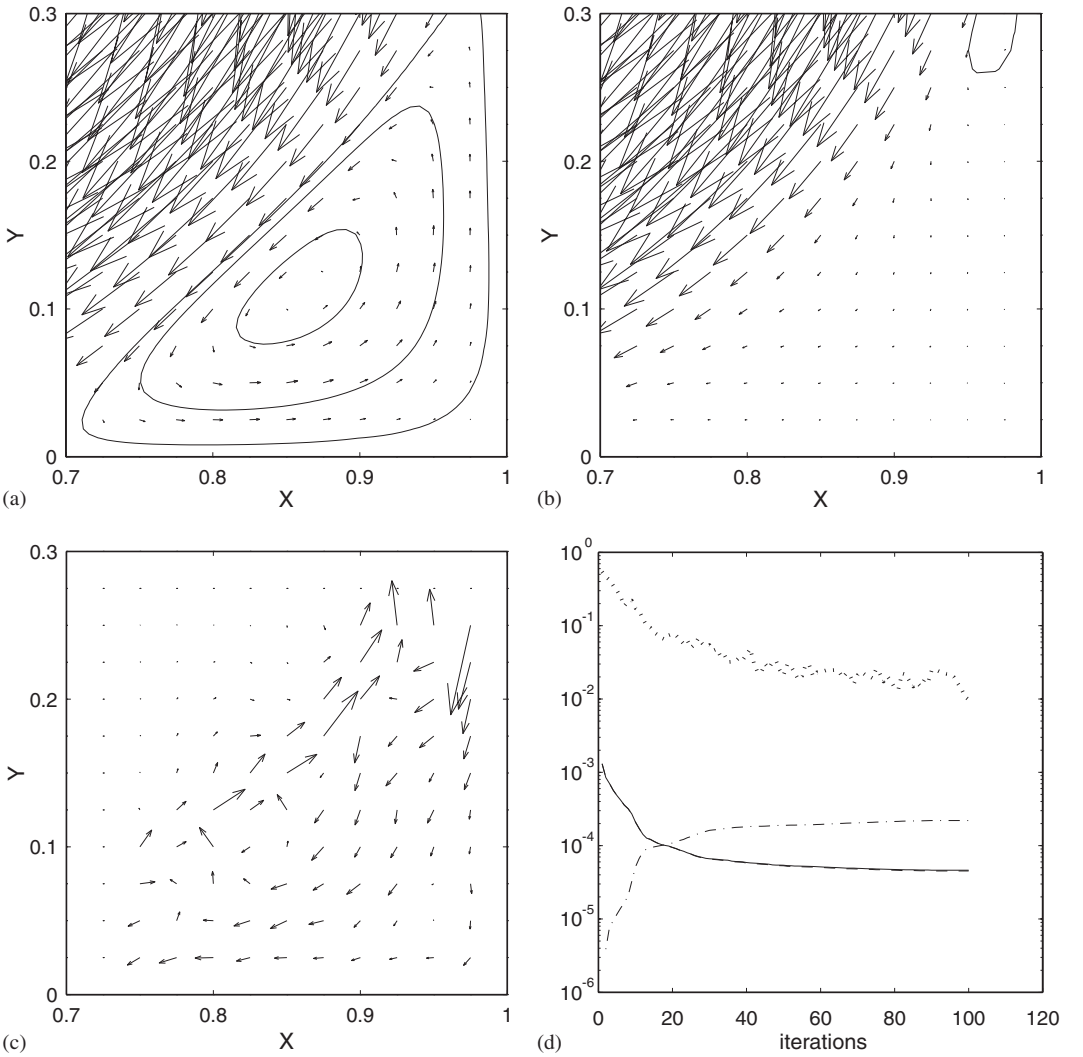

Figure 6. Results for $Re = 1000$ and $\varepsilon = 1$: (a) uncontrolled flow: levels of Ψ $[5 \times 10^{-5}, 5 \times 10^{-4}, 1.5 \times 10^{-3}]$ and velocity vectors; (b) controlled flow: a level of Ψ $[5 \times 10^{-5}]$ and velocity vectors at $t = 0.8$ (note that the levels of Ψ are not present in Ω_o because of the reduction of Ψ); (c) control force at $t = 0.8$; and (d) convergence with the number of CG iterations: — J, -- J_1, $\cdot$– $J_2, \cdots \|\nabla J\|$.

vortex reduction strategies. The optimality system and the gradient of the cost with respect to the control are characterized and a possible numerical realization is proposed. It efficiency is demonstrated by two-dimensional numerical examples. The results that were obtained on the basis of new cost functional encourage further analysis of the proposed techniques to boundary control, different geometries and three-dimensional problems.

REFERENCES

1. Desai M, Ito K. Optimal control of Navier–Stokes equations. *SIAM Journal on Control and Optimization* 1994; **32**:1428–1446.
2. Abergel F, Temam R. On some control problems in fluid mechanics. *Theoretical and Computational Fluid Dynamics* 1990; **1**:303–325.
3. Berggren M. Numerical solution of a flow conrtol problem: vorticity reduction by dynamic boundary action. *SIAM Journal on Scientific Computing* 1998; **19**:829–860.
4. Casas E. Optimality conditions for some control problems of turbulent flows. In *Flow Control*, Gunzburger M (ed.). Springer: Berlin, 1995.
5. Jeong J, Hussain F. On the identification of a vortex. *Journal of Fluid Mechanics* 1995; **85**:69–94.
6. Alen BG. Distributed feedback control for flow in a driven cavity. *ICASE Research Quarterly* 2000; **9**: http:www.icase.edu/RQ/art2.html.
7. Cattafesta LN, Garg S, Choudhari M, Li F. Active control of flow-induced cavity resonance. *AIAA Paper* 97-1804, 1997.
8. He JW, Glowinski R, Metcalfe R, Nordlander A, Periaux A. Active control and drag reduction for flow past a circular cylinder. I. Oscillatory cylinder rotation. *Journal of Computational Physics* 2000; **163**:83–117.
9. Park HM, Lee WJ, Chung JS. Boundary optimal control of the Navier Stokes equations—a numerical approach. *International Journal of Engineering Sciences* 2002; **40**:2119–2135.
10. Borggaard J, Burns J, Cliff E, Schreck S. *Computational Methods for Optimal Design and Control*. Birkhäuser: Boston, 1998.
11. Gunzburger M. *Flow Control*. Springer: New York, 1995.
12. Kaplan W. *Ordinary Differential Equations*. Addison-Wesley Publ. Comp.: Reading, MA, 1967.
13. Chong MS, Perry AE, Cantwell BJ. A general classification of three-dimensional flow fields. *Physics of Fluids A* 1990; **2**:765–777.
14. Blackburn HM, Monsour NN, Cantwell BJ. Topology of fine-scale motions in turbulent channel flow. *Journal of Fluid Mechanics* 1996; **310**:293–324.
15. Perry AE, Chong MS. A description of eddying motions and flow patterns using critical-point concepts. *Annual Review of Fluid Mechanics* 1987; **19**:125–155.
16. Hunt JCR, Wray AA, Moin P. Eddies, stream and convergence zones in turbulent flows. *Center for Turbulence Research Report* CTR-S88, 193 ff, 1988.
17. Geiger C, Kanzow C. *Numerische Verfahren zur Lösung unrestringierter Optimierungsaufgaben*. Springer: Berlin, 1999.
18. Moré JJ, Sorensen DC. Newton's method. In *Studies in Numerical Analysis*, Golub GH (ed.). The Mathematical Association of America, Washington, DC, USA, 1984; 29–82.
19. Gilbert JC, Nocedal J. Global convergence properties of conjugate gradient methods for optimization. *SIAM Journal on Optimization* 1992; **2**:21–42.
20. Powell MJD. Nonconvex minimization calculation and the conjugate gradient method. In *Lecture Notes on Mathematics*, vol. 1066. Springer: Berlin, 1984; 122–141.
21. Gill PE, Murray W, Wright MH. *Practical Optimization*. Academic Press: San Diego, 1981.
22. Ghia U, Ghia KN, Shin CT. High-resolutions for incompressible flow using the Navier–Stokes equations and a multigrid method. *Journal of Computational Physics* 1982; **48**:387–411.
23. Leriche E, Gavrilakis S. Direct numerical simulation of the flow in a lid-driven cavity flow. *Physics of Fluids* 2000; **12**:1363–1376.
24. Patankar SV. *Numerical Heat Transfer and Fluid Flow*. McGraw-Hill: New York, 1980.
25. Gollub GH, Van Loan ChF. *Matrix Computations* (3rd edn). The Johns Hopkins University Press: Baltimore, 1996.
26. Bewley TT. Flow control: new challenges for a new Renaissance. *Progress in Aerospace Sciences* 2001; **37**:21–58.
27. Choi H, Hinze M, Kunisch K. Instantaneous control of backstep-facing step flows. *Applied Numerical Mathematics* 1999; **31**:133–158.

